Journal of
Nanoscience and Nanotechnology
Vol. 12, 5747–5753, 2012

RESEARCH ARTICLE

Enhanced Light Output from the Nano-Patterned InP Semiconductor Substrate Through the Nanoporous Alumina Mask

Mi. Jung[1], Jae Hun Kim[1], Seok Lee[1], Byung Jin Jang[2], Woo Young Lee[2], Yoo-Mi Oh[3], Sun-Woo Park[3], and Deokha Woo[1,*]

[1] *Sensor System Research Center, Korea Institute of Science and Technology, Seoul 136-791, Republic of Korea*
[2] *Department of Materials Science and Engineering, Yonsei University, Seoul 120-749, Korea Seoul 136-791, Republic of Korea*
[3] *Department of Electrical and Computer Engineering, University of Seoul, Seoul 130-743, Republic of Korea*

A significant enhancement in the light output from nano-patterned InP substrate covered with a nanoporous alumina mask was observed. A uniform nanohole array on an InP semiconductor substrate was fabricated by inductively coupled plasma reactive ion etching (ICP-RIE), using the nanoporous alumina mask as a shadow mask. The light output property of the semiconductor substrate was investigated via photoluminescence (PL) intensity measurement. The InP substrate with a nanohole array showed a more enhanced PL intensity compared with the raw InP substrate without a nanohole structure. After ICP-RIE etching, the light output from the nanoporous InP substrate covered with a nanoporous alumina mask showed fourfold enhanced PL intensity compared with the raw InP substrate. These results can be used as a prospective method for increasing the light output efficiency of optoelectronic devices.

Keywords: Light Output Efficiency, InP Nanohole, Photoluminescence, Nanoporous Alumina Mask.

1. INTRODUCTION

The light output property of a semiconductor substrate with nanoholes is very attractive for future applications in optoelectronic devices. Indium phosphide (InP), as a typical III–V compound semiconductor, is a promising material for use in high-speed optoelectronic devices due to its high electron mobility and direct band gap.[1] Owing to its optical properties, InP is also a very important material for solid-state optical devices such as solar cells, semiconductor lasers, and light-emitting diodes (LEDs).[2–5] Due to its direct bandgap (1.34 eV), InP is very suitable for solar cells.[3] Solar cells using InP have been found to have higher conversion efficiency and higher radiation resistance than other semiconductors.[4] Semiconductor lasers with wavelengths in the eye-safer region have advantages in medical applications.[5] They are especially useful in medical equipment where the signals from a low-voltage sensor circuit are in contact with a living organism. Infrared LEDs are also used as light sources for many sensor systems. The infrared LED, a type of electronic device that emits infrared light (> 700 nm), may be used for remote control, to transfer data among electronic devices, medical equipment, and many other domestic appliances. In the conventional LEDs, light extraction is limited by the total internal reflection. The photons generated inside the LED are reflected back into the semiconductor layer because of the high refraction index difference at the semiconductor/air surface interface.[6] Thus, the textured surface structure of semiconductor devices is very important for the improvement of the light extraction efficiency.[6]

To extract more light from the semiconductor surface, various surface-texturing methods including surface roughening via laser etching[7] or the laser lift-off technique,[8] fabrication of a photonic bandgap crystal by laser holography[9] or anodization,[10,11] and creation of a nano-patterned surface using nanomaterials via dry etching,[12,13] have been proposed. To utilize the uniform channels of the nanometer dimensions, a self-organized nanoporous alumina layer has been used as a shadow mask for a pattern with a nanometer size on the surface of the semiconductor substrate.[14–16] The nanoporous alumina layers have been

*Author to whom correspondence should be addressed.

 1533-4880/2012/12/5747/007 doi:10.1166/jnn.2012.6252

widely used as templates for the fabrication of nanodot arrays, nanowires, and other nanostructures for many applications.[17–21] Relatively little research work has been done, however, on the property of the light output from a nano-patterned substrate covered with a nanoporous alumina mask.

Reported in this letter is the work on the fabrication and optical property of a size- and density-controlled semiconductor nanohole array on an InP substrate using nanoporous alumina as a shadow mask. Nanoholes were fabricated on the surface of an InP semiconductor substrate by inductively coupled plasma reactive ion etching (ICP-RIE), using the nanoporous alumina mask. The light output property of the substrate with nanoholes was studied via photoluminescence (PL) intensity measurement.

2. EXPERIMENTAL DETAILS

Well-ordered nanoporous alumina layers were prepared from an aluminum foil (99.99%, 100 μm thick) by two-step anodization.[18] The first anodization was performed by applying the DC voltage of 40 V in 0.3 M oxalic acid or 24 V in 0.3 M sulfuric acid, and the electrolyte was vigorously stirred and maintained at 3 °C in a circulator system. The alumina layer formed in the first anodization was completely dissolved in mixture solution of phosphoric acid (0.4 M) and chromic acid (0.2 M) at 65 °C for several hours. The second anodization process was conducted under the same condition as in the first anodization, but with a different anodization time. For the preparation of the through-hole nanochannel alumina masks, two-time chemical wet-etching processes were used, which involved dipping the aluminum oxide layer twice in the chemical-etching solution, a process described in detail elsewhere.[20] After the second anodization, the alumina layer was slightly etched via immersion for 5–9 min in aqueous 5 wt% phosphoric acid at 30 °C. Then the surface of the nanoporous alumina mask was coated with a protective layer, and the remaining aluminum was removed in saturated $HgCl_2$ solution. The alumina layer was etched again for 5–7 min in aqueous 5 wt% phosphoric acid. The protective layer was dissolved in acetone and was rinsed several times in distilled water. Finally, the nanoporous alumina mask with through-holes was placed on the surface of an InP substrate. The InP wafer supplied by ACROTEC® was used in this experiment.[22]

The InP substrate with an alumina mask on its surface was subsequently placed on the cathode electrode of the ICP-RIE system. Under the ICP source power of 1500 W and the RF bias power of 100 W, the InP substrate was etched in the fixed flow rate ratio (7:8:9) of Cl_2, CH_4, and H_2 gases. Under these ICP-RIE conditions, the InP substrate was etched at the rate of 1.89 μm/min. After the ICP-RIE process, the alumina mask on the surface of the semiconductor substrate was dissolved for several hours in the mixture of phosphoric acid and chromic acid at 65 °C. The morphologies of the alumina layer and the nanoholes on the semiconductors were observed using a field emission scanning electron microscope (FESEM). The PL spectra of the samples were observed through excitation with a 514 nm Ar-ion laser source at room temperature. The incident power of Ar ion laser was varied from 30 to 60 mW.

3. RESULTS AND DISCUSSION

Anodic aluminum oxide (AAO) is formed on the aluminum substrate connected to the anode of a power supply by anodization process and by applying a constant bias voltage to an acidic solution such as sulfuric or oxalic acid. Figure 1(a) shows a schematic diagram of aluminum oxide layer fabricated by this anodization process. The structure of AAO consists of a barrier layer and a porous alumina layer.[23] The structure of the barrier layer consists of aluminum oxide (=alumina) formed with a concaved pattern on the aluminum substrate. The structure of the porous alumina layer consists of the aluminum oxide of a hexagonally close-packed array with nanosized cylindrical pores perpendicular to the surface of the aluminum substrate. The cell size and the interpore distance of the hexagonally close-packed nanoporous array are linearly dependent on the anodization voltage.[23, 24] Well-ordered AAO was prepared from aluminum using the two-step anodization process.[18] After removing the AAO formed at the first anodization process, a second anodization process was conducted for 4 min under the same conditions as in the first anodization. Figure 1(b) presents the FESEM image of the oblique view of the alumina layer, which was formed by applying a constant DC voltage of 40 V in a 0.3 M oxalic acid solution for 4 min. The thickness of the nanoporous alumina layer fabricated at the anodization time of 4 min was about 200 nm. The thickness of the nanoporous alumina layer can be controlled by varying the anodization time considering the dependency between the different growth rates on the voltage and the electrolyte.[22] Further, the cell size and pore density of the AAO are dependent on the anodization voltage. After the second anodization, the remaining aluminum substrate was removed in a saturated $HgCl_2$ solution. Figure 2(a) shows the cell base pattern of the AAO prepared at 25 V in 0.3 M sulfuric acid. As shown in Figure 2(a), the distance between the cells and the pore density of the AAO prepared at 25 V were 66 ± 4 nm and 2.8×10^{10} cm^{-2}, respectively. The cell base of the AAO was arranged in a hexagonal close packed pattern. In Figure 2(b), the pore size of the AAO after the second anodization is shown to be 16 ± 3 nm. Figure 2(c) shows the pore diameter widened by dipping the AAO in a 5 wt% solution of H_3PO_4 for 30 min at 30 °C. The pore diameter is 45 ± 3 nm. Figure 2(d) shows the cell base pattern of the AAO prepared at 40 V in 0.3 M oxalic acid. The distance between the cells and the pore density of the AAO prepared at 40 V

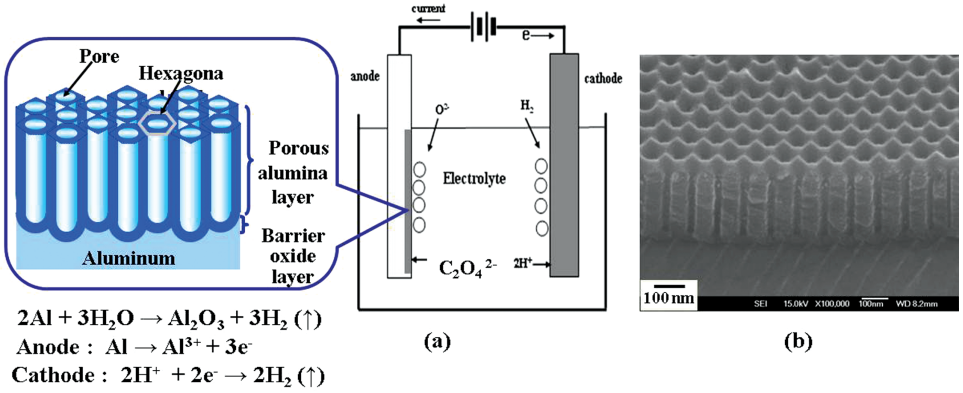

Fig. 1. (a) Schematic illustration of the anodization and structure of the aluminum oxide layer on aluminum. (b) FESEM image of the aluminum oxide layer prepared at the anodization voltage of 40 V in 0.3 M oxalic acid for 4 min.

are shown to be 105 ± 5 nm and 1.0×10^{10} cm^{-2}, respectively. In Figure 2(e), the pore size of the AAO after the second anodization is shown to be 30 ± 3 nm. Figure 2(f) shows the shape of the widened pore diameter by dipping in a 5 wt% H_3PO_4 solution for 30 min at 30 °C. The pore diameter was 60 ± 4 nm. The pore diameter was adjustable within the range of the hexagonal cell size of the AAO, by varying the widening time.

It was confirmed that the alumina barrier layer at the bottom of the AAO was removed thoroughly in the second etching process. The thickness of the alumina mask with through-holes was approximately 200 nm. The mask with a thickness of ca. 200 nm was bonded on the InP substrate surface by the van der Waals force.[19] ICP-RIE was conducted on the InP substrate with a nanoporous alumina mask on its surface for various etching times. The surface of the nanoporous alumina mask etched via ICP-RIE and the nanohole array on the surface of the InP substrate are shown in Figure 3. The substrate covered with the nanoporous alumina mask was exposed to the ion bombardment induced by ICP-RIE under the fixed flow rate ratio (7:8:9) of Cl_2, CH_4, and H_2 gases for 30 sec. The FE-SEM images of the top and oblique views of the alumina mask bonded on the InP substrate after the ICP-RIE are shown in Figures 3(a) and (d). The InP substrate was etched for 30 sec via ICP-RIE, using the nanoporous alumina mask. Then the nanoporous alumina mask bonded on InP substrate was dissolved out in chemical etching solution. The nanohole array that was formed on the InP substrate after removal of the nanoporous alumina mask prepared at 40 V in 0.3 M oxalic acid is shown in Figure 3(c). The surface morphology of the nanohole array on the InP substrate shows that the average pore diameter and the pore density of the InP substrate were 45 ± 5 nm and 0.9×10^{10} cm^{-2}, respectively. The FESEM images of the top and oblique views of the nanoporous alumina mask etched via ICP-RIE for 60 sec are shown in Figures 3(b) and (e). In Figure 3(e), the interface between the InP

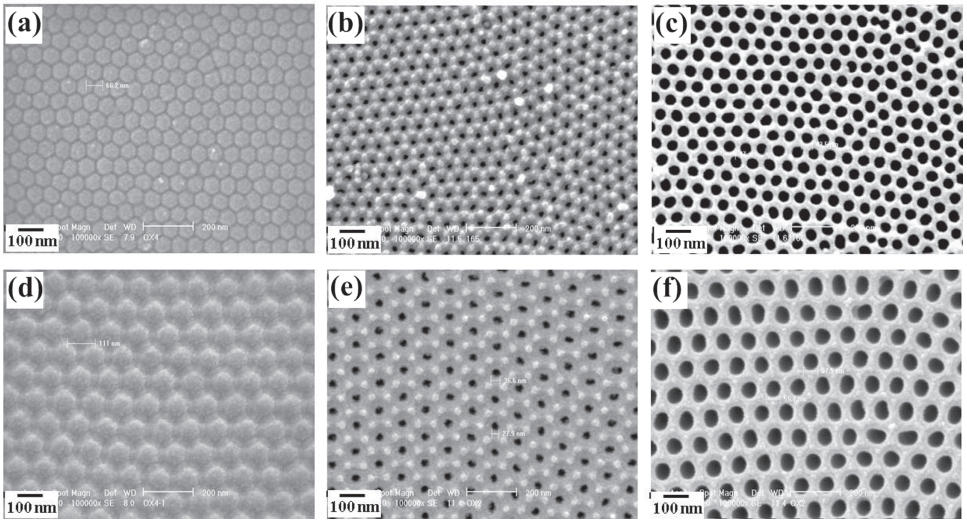

Fig. 2. FESEM images: (a) Cell base pattern and (b) top-view of aluminum oxide layer prepared at 25 V in 0.3 M sulfuric acid; (c) pore diameter variation by dipping for 30 min in phosphoric acid; (d) cell base pattern and (e) top-view of aluminum oxide layer prepared at 40 V in 0.3 M oxalic acid; and (f) pore diameter variation carried out by dipping in 5 wt% H_3PO_4 at 30 °C for 30 min.

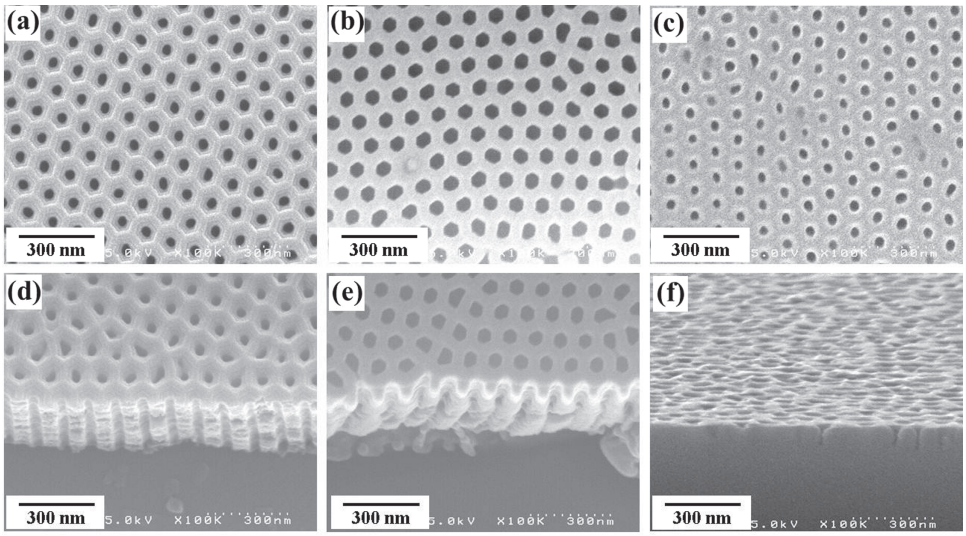

Fig. 3. FESEM images of top view of the nanoporous alumina mask etched via ICP-RIE for (a) 30 sec and (b) 60 sec, of (c) the nanoporous InP substrate etched via ICP-RIE for 30 sec, whose mask was removed in a chemical solution. FESEM images of the oblique view of the nanoporous alumina etched via ICP-RIE for (d) 30 sec and (e) 60 sec, and of (f) the nanoporous InP substrate etched via ICP-RIE for 30 sec. The alumina mask was prepared at 40 V in 0.3 M oxalic acid at 3 °C.

substrate and the nanoporous alumina mask was etched via ICP-RIE for 60 sec. The effect of the ion bombardment induced by inductively coupled plasma responded properly on the InP substrate through the alumina mask. The alumina mask showed high tolerance to the ion bombardment induced by ICP-RIE.

To make an AAO mask with a higher density and smaller pores, the AAO was prepared through a second anodization at 25 V in 0.3 M sulfuric acid for 150 sec. After the second anodization, the AAO was slightly etched via immersion in aqueous 5 wt% phosphoric acid for 5 min at 30 °C. Then the remaining aluminum substrate was removed in saturated $HgCl_2$ solution. The AAO was dipped again for 5 min in aqueous 5 wt% phosphoric acid. The nanoporous alumina mask with through-hole of smaller-diameter through holes was placed on the InP substrate. Figure 4(a) shows FESEM image of the top-view of the nanoporous alumina mask exposed to the ion bombardment induced by ICP-RIE for 90 sec. As shown in Figure 4(a), the nanoporous alumina mask was damaged by the ion bombardment induced by ICP-RIE. The InP substrate was etched for 15 sec by ICP-RIE, using the nanoporous alumina mask prepared at 25 V. Then the alumina mask was dissolved out in chemical-etching solution. The nanohole array that was formed on the InP substrate after removal of the nanoporous alumina mask is shown in Figure 4(b). Although etched for 15 sec by ICP-RIE using the alumina mask, the nanohole array on the InP substrate was not well formed. The configuration of the nanohole array on the InP substrate after etching for 30 sec via ICP-RIE using the alumina mask can be clearly seen in Figure 4(c). The ion bombardment induced by ICP-RIE responded properly on the InP substrate through the nanoholes of the alumina mask. The uniform array of nano-sized pores produced in the alumina mask was successfully transferred to the InP substrate. At a low anodization voltage in sulfuric acid, a nanoporous alumina mask with a high pore density can be prepared. A nanohole array was formed on the InP substrate with an average pore density of about 2.6 $(\pm 0.2) \times 10^{10}$ cm^{-2}, as shown in Figure 4(c). The average diameter of holes on the InP substrate was 30 ± 5 nm. The nanohole configuration on the InP substrate depended on the hole morphology of the alumina mask and the etching time by ICP-RIE.

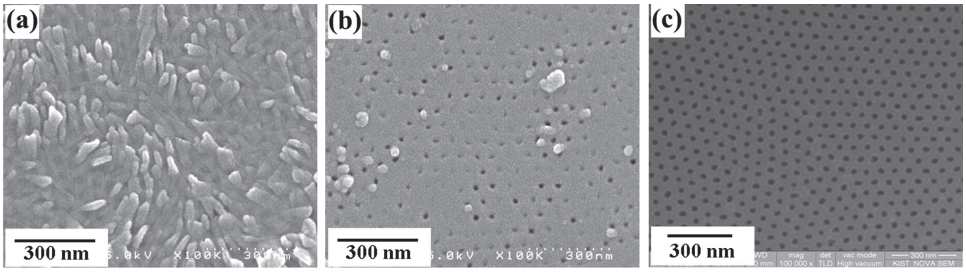

Fig. 4. FESEM images of the top views of the (a) alumina mask etched for 90 sec; (b) nanohole array on the InP substrate etched for 15 sec; and (c) nanohole array on the InP substrate etched for 30 sec via ICP-RIE using the alumina mask prepared at 25 V in 0.3 M sulfuric acid.

The light emission property from the InP substrate with a nanohole array was studied by PL intensity measurement at room temperature. Figure 5(a), the PL intensity from the nanohole array on the InP substrate is shown to have been enhanced compared with that from the InP substrate without such structure. The emission spectra of the nanohole array on the InP substrate showed a broad peak centered at 932 nm. After all, the peak position obtained from the nanohole array on the InP substrate did not shift from the InP substrate without such structure. The PL spectra were observed via the excitation with a 514 nm Ar-ion laser source at the incident power of 40 mW.

The nature of the InP band gap has been discussed by many researchers.[25–27] PL emission bands give information about the electronic states in the gap of InP substrate. It is often difficult to determine the exact origins of these states due to various types of imperfections, such as the vacancies and atoms on surfaces, because they may be very close in the luminescence bands.[28] The band gap of undoped InP is 1.35 eV at room temperature.[25, 26] The PL peak is attributed to a superposition of the conduction band-to-valence band (CV) transition and the shallow donor-valence band (DV) transition.[24] The DV transition shows itself at around 7–10 meV below the CV peak.[27]

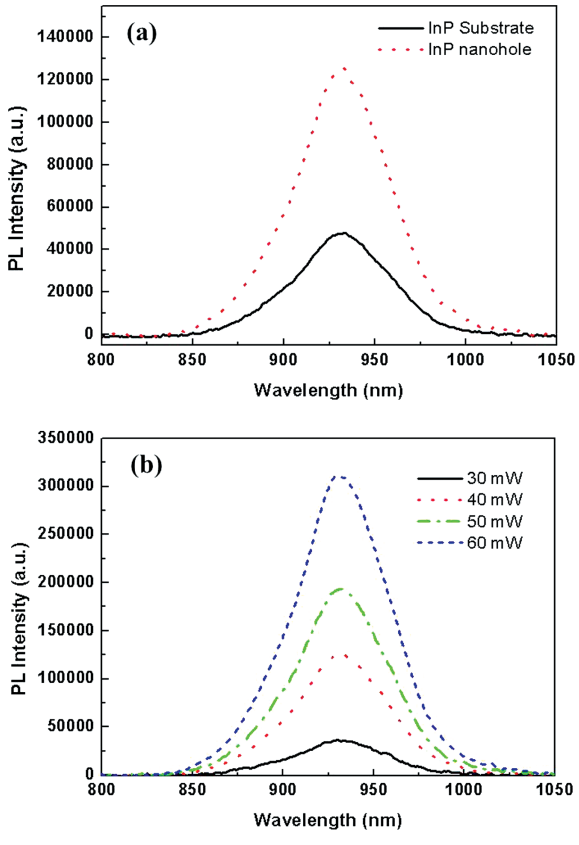

Fig. 5. PL spectra of (a) the InP substrate and nanohole array formed on the InP substrate using the alumina mask prepared at 40 V in 0.3 M oxalic acid at 3 °C, and of (b) the nanohole array measured with different laser powers.

It was recently reported that the emission photon energy of the *n*-InP substrate was near 1.3 eV at room temperature for a carrier concentration of $n = 2 \times 10^{18}$ cm^{-3}.[2] At room temperature, PL intensity measurement over a range of optical powers was performed on the same sample of nanohole array formed on the InP substrate, using the alumina mask prepared at 40 V in 0.3 M oxalic acid. Figure 5(b) shows the PL spectra that were measured at different laser powers. The PL intensity of the emission bands centered at 932 nm was enhanced by varying the laser power. The peak positions did not shift while the laser power was varied from 30 to 60 mW.

To further compare the improvement of the light extraction by the nanohole array, the ligh extraction from three different samples was investigated: the bare InP substrate, the InP nanohole substrate, and the AAO mask/InP nanohole substrate. The AAO mask/InP nanohole substrate was prepared by etching the InP substrate with a nanoporous alumina mask. The InP nanohole substrate was obtained by removing the alumina mask from the previous sample. The nanohole array was formed on the InP substrate for 30 sec via ICP-RIE, using the nanoporous alumina mask prepared at anodization voltage of 25 V in 0.3 M sulfuric acid. Figure 6(a) shows the FESEM image of the top views of the nanoporous alumina mask and nanohole array formed on the InP substrate. Figure 6(b) shows the room temperature PL spectra measured from the bare InP substrate, from the InP substrate with a nanohole array, and from InP substrate with both a nanoporous alumina mask and a nanohole array. The PL peak at 932 nm from the InP substrate was due to the band edge wavelength of the *n*-InP substrate. After all, the peak position at 932 nm did not shift, and the spectral width was almost the same in the three samples. The PL intensity from the triangular array of air cylinders with nanoholes on the InP substrate showed threefold enhancement in comparison with that from the bare InP substrate without such structure. Furthermore, the PL intensity from the InP substrate with both a nanoporous alumina mask and a nanohole arrays showed forefold enhancement compared with that from the bare InP substrate. Thses results revealed that the InP substrate with nanoholes using a nanoporous alumina mask showed much enhanced emission compared with the surface of the porous InP structure without a nanoporous alumina mask, resulting in the increased probability of photon escape from the ordered structure.[11]

The nanopores formed on the surface of the InP substrate induced the enhancement of the PL intensity from the semiconductor. It seems that the nanoporous alumina with the refraction index of 1.67 can reduce the difference of the refraction indices of InP ($n = 3.1$) and air ($n = 1.0$). Therefore, the light from the InP substrate covered with the nanoporous alumina mask was more enhanced by both the surface roughness of the InP substrate and the mid index layer. After ICP-RIE etching, no PL spectrum

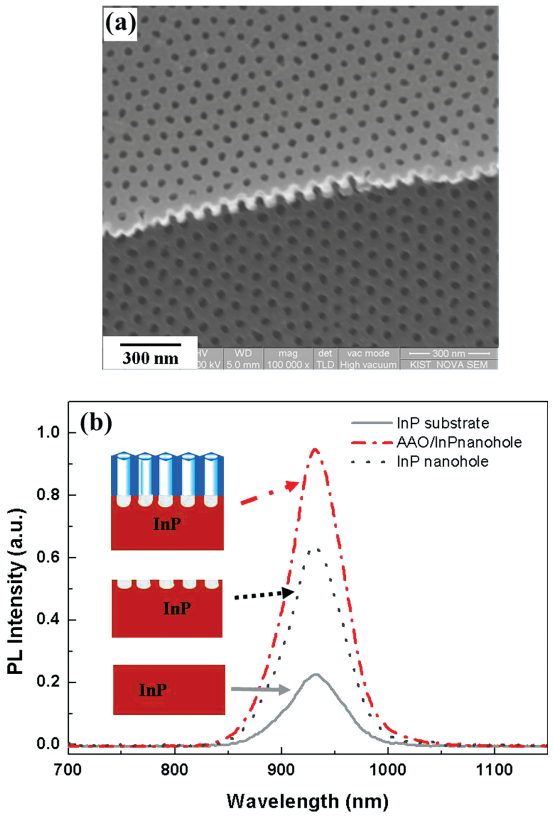

Fig. 6. (a) FESEM image of the top views of the alumina mask and nanohole array formed on the InP substrate for 30 sec by ICP-RIE using the alumina mask prepared at the anodization voltage of 25 V in 0.3 M sulfuric acid; (b) PL spectra measured from the InP substrate, the alumina mask on the nanohole array, and the nanohole array formed on the InP substrate.

was obtained from the InP substrate without well-formed nanohole array. It is reported that the PL intensity of the band edge is sensitive to plasma-induced damage,[29] but in the case where the InP substrate is covered with a nanoporous alumina mask after ICP-RIE etching, the PL intensity showed more enhancement compared with that from the bare InP substrate. The nanohole array on the InP semiconductor provides angulrrandomization of the total internal reflection, depresses total internal reflection and contributes to the efficient light extraction from the semiconductor to the air. The internal light generated inside the semiconductor can efficiently escape into the air through the nanooporous alumina mask and the nanohole array on the surface of semiconductor substrate. The nanoporous alumina mask can be used to provide the appropriate surface texturing for enhancing the light extraction efficiency without reducing the other optical properties of the semiconductor in optoelectronic devices.

4. CONCLUSIONS

In this work, a nanohole arrays was fabricated on an InP substrate via inductively coupled plasma reactive ion etching (ICP-RIE) with a nanoporous alumina mask. The shape of the nanoholes on the InP substrate depended on the etching time, and the pattern of the alumina mask was controlled by the anodization condition. The average hole diameter of the nanohole array formed on the InP substrate via ICP-RIE for 30 sec by utilizing alumina mask prepared at an anodization voltage of 25 V in 0.3 M sulfuric acid solution was 30 ± 5 nm. The light output property of the InP substrate with nanohole roughening was studied via photoluminescence (PL) intensity measurement. The emission bands centered at 932 nm (1.3 eV) from the InP substrate covered with both nanoholes and a nanoporous alumina mask showed fourfold enhancement compare with that from the bare InP substrate. The peak position obtained from the InP substrate with a nanohole array did not shift from that obtained from the InP substrate without such structure. The nanoporous alumina mask with a medium refraction index can reduce the refraction index difference between the InP substrate and the air. Therefore, it seems that the light from the InP substrate covered with a nanoporous alumina mask was enhanced both by the surface roughness of the InP substrate and by the medium-refraction-index layer. The ICP-RIE technique using a nanoporous alumina mask can be used as a prospective method for increasing the light output of light-emitting diodes via nanohole surface roughening.

Acknowledgments: This study was supported by the Public Welfare and Safety Research Program through a National Research Foundation of Korea (NRF) grant funded by the Ministry of Education, Science, and Technology (MEST, 2011-0020953).

References and Notes

1. Z. W. Deng, R. W. M. Kwok, W. M. Lau, and L. L. Cao, *Appl. Surf. Sci.* 158, 58 (**2000**).
2. O. Semyonov, A. Subashiev, Z. Chen, and S. Luryi, *J. Appl. Phys.* 108, 013101 (**2010**).
3. K. Ito and T. Nakazawa, *J. Appl. Phys.* 58, 2639 (**1985**).
4. M. Yamguchi and K. Ando, *J. Appl. Phys.* 63, 5555 (**1988**).
5. T. Stakelon, J. Lucas, M. Osowski, R. Lammert, S. Moon, C. Panja, V. Elarde, K. Gallup, and W. Hu, *J. Ungar SPIE* 7198, 719819 (**2009**).
6. R. H. Horng, C. C. Yang, J. Y. Wu, S. H. Huang, C. E. Lee, and D. S. Wuu, *Appl. Phys. Lett.* 86, 221101 (**2005**).
7. H.-W. Huang, J. T. Chu, C. C. Kao, T. H. Hseuh, T. C. Lu, H. C. Kuo, S. C. Wang, and C. C. Yu, *Nanotechnology* 16, 1844 (**2005**).
8. T. Fujii, Y. Gao, R. Sharma, E. L. Hu, S. P. D. Baars, and S. Nakamura, *Appl. Phys. Lett.* 84, 855 (**2004**).
9. D.-H. Kim, C.-O. Cho, Y.-G. Roh, H.-S. Jeon, Y.-S. Park, J.-H. Cho, J.-S. Im, C.-S. Sone, Y.-J. Park, W.-J. Choi, and Q.-H. Park, *Appl. Phys. Lett.* 87, 203508 (**2005**).
10. T. Baba and M. Koma, *Jpn. J. Appl. Phys.* 34, 1405 (**1995**).
11. T. Takizawa, S. Arai, and M. Nakahara, *Jpn. J. Appl. Phys.* 33, L643 (**1994**).
12. H. Gong, X. Hao, W. Xia, Y. Wu, and X. Xu, *Eur. Phys. J. Appl. Phys.* 50, 10301 (**2010**).

13. M.-Y. Hsieh, C.-Y. Wang, L.-Y. Chen, T.-P. Lin, M.-Y. Ke, Y.-W. Cheng, Y.-C. Yu, C.-P. Chen, D.-M. Yeh, C.-F. Lu, C.-F. Huang, C.-C. Yang, and J.-J. Huang, *IEEE Electron Devices Lett.* 29, 658 **(2008)**.
14. K.-J. Kim, J.-H. Choi, T.-S. Bae, M. Jung, and D.-H. Woo, *Jpn. J. Appl. Phys.* 46, 6682 **(2007)**.
15. C. Huh, K.-S. Lee, E.-J. Kang, and S.-J. Park, *J. Appl. Phys.* 93, 9383 **(2003)**.
16. M. Jung, S. Lee, Y.-M. Jhon, S.-I. Mho, J.-W. Cho, and D. H. Woo, *Jpn. J. Appl. Phys.* 46, 4410 **(2007)**.
17. M. Nakao, S. Oku, T. Tamamura, K. Yasui, and H. Masuda, *Jpn. J. Appl. Phys.* 38, 1052 **(1999)**.
18. H. Masuda and M. Satoh, *Jpn. J. Appl. Phys.* 35, L126 **(1996)**.
19. X. Mei, M. Blumin, D. Kim, Z. H. Wu, and H. E. Ruda, *J. Cryst. Growth* 251, 253 **(2003)**.
20. M. Jung, W. A. El-Said, and J.-W. Choi, *Nanotechnology* 22, 425203 **(2011)**.
21. M. Jung, W. A. El-Said, B.-K. Oh, and J.-W. Choi, *J. Nanosci. Nanotechnol.* 11, 4205 **(2011)**.
22. ACROTEC Inc, Japan, www.Acrotec.com.
23. F. Keller, M. S. Hunter, and D. L. Robinson, *J. Electrochem. Soc.* 100, 411 **(1953)**.
24. A. P. Li, F. aMuller, A. Briner, K. Nielsch, and U. Gosele, *J. Appl. Phys.* 84, 6023 **(1998)**.
25. R. E. Nahory, M. A. Pollack, R. L. Barns, and W. D. Johnston, *Appl. Phys. Lett.* 33, 659 **(1978)**.
26. L. Pavesi, F. Piazza, A. Rudra, J. F. Carlin, and M. Ilegems, *Phys. Rev. B* 44, 9052 **(1991)**.
27. I. Tsimberova, Y. Rosenwaks, and M. Molotskii, *J. Appl. Phys.* 93, 9797 **(2003)**.
28. D. Denzler, M. Olschewki, and K. Sattler, *J. Appl. Phys.* 84, 2841 **(1998)**.
29. S. Tripathy, A. Ramam, S. J. Chua, J. S. Pan, and A. Huan, *J. Vac. Sci. Technol. A* 19, 2522 **(2001)**.

Received: 2 August 11. Accepted: 12 January 2012.